

All-gas-phase Synthesis and Functionalization of Silicon Nanocrystals

Z. Li and U. Kortshagen

Department of Mechanical Engineering, University of Minnesota, Minneapolis, Minnesota, USA

Abstract: Nonthermal plasma synthesis allows continuous production of high purity silicon nanocrystals. Here we present an all-gas-phase synthesis route that produces highly luminescent silicon nanocrystals. Photoluminescence quantum yields of the as-produced silicon nanocrystals exceeds 20%, which is a five-fold increase compared with previous all-gas-phase approaches. The increased PLQY is concurrent with reduced SiH_3 species during the in-flight heating step.

Keywords: silicon, nanocrystals, nonthermal plasma, photoluminescence, ligands

1. Introduction

Silicon nanocrystals (Si NCs) are promising materials for light-emitting applications including luminescent solar concentrators [1], light emitting devices [2,3] and biomedical applications [4,5] due to their earth abundance, biocompatibility, and low toxicity [6,7]. Among the methods of Si NC synthesis, nonthermal plasma synthesis is attractive because it allows continuous production of nanocrystals while eliminating the need for excessive solvents and ligands [8]. Unfortunately, as-produced, plasma-synthesized Si NCs usually have low photoluminescence quantum yield (PLQY). For light-emitting applications, higher PLQY is desired in order to achieve better device performance. In order to improve PLQY of Si NCs, post-processing is necessary, which is usually done via hydrosilylation after Si NC synthesis. Hydrosilylation can be initiated either thermally [9], photochemically [10], by applying a catalyst [11], or using bifunctional ligands [12]. Each of these methods are conducted post-synthesis and require additional processing steps.

Previous studies have demonstrated the feasibility of gas-phase functionalization of Si NCs. Integrated with non-thermal synthesis, these designs could potentially overcome the disadvantages of post-synthesis functionalization. A plasma-assisted functionalization route was developed by Mangolini *et al.* in which the nanoparticles together with ligands enter a second plasma chamber after the main synthesis plasma [13]. Anthony *et al.* improved this scheme by combining synthesis and functionalization in two spatially separated regions of a single plasma [14], which has the advantage that nanocrystals never leave the plasma between their synthesis and functionalization and remain in a negatively charged state that prevents nanocrystal aggregation. In both experiments, however, PLQY remained low at less than 5% even though ligands were successfully grafted onto Si NC surfaces.

In this study, we present an all-gas-phase synthesis and functionalization route for silicon nanocrystals with > 20% photoluminescence quantum yield. Based on the work of

Anthony *et al.* [14], Si NCs are synthesized and functionalized with ligands in a single plasma. The NC synthesis was achieved in a higher density upstream synthesis region and functionalizing ligands were injected downstream into the lower density plasma “afterglow”, where the density of plasma species decays through recombination. The residence time of Si NCs in the synthesis and the functionalization zones is on the order of milliseconds. However, different from previous work, Si NCs then enter a flow-through furnace, where they are heated in-flight. The characteristic time for the NC temperature to equilibrate with the gas temperature through conduction is only on the order of 0.01 milliseconds due to the small heat capacitance of the 2-4 nm Si NCs, even considering the low-pressure environment at which the Knudsen effect becomes significant. By letting the aerosol stream of Si NCs flow through a tube furnace after the plasma synthesis region, the temperature of Si NCs will closely follow the gas temperature profile in the furnace. As shown below, this in-flight heating during which the residence time is only ~100 milliseconds significantly improves the nanocrystal PLQY. Hence, with this all-gas-phase design, highly luminescent Si NCs are synthesized on a timescale of 100 milliseconds, which is orders of magnitude faster than schemes that require liquid post-synthesis processing.

2. Experimental Details

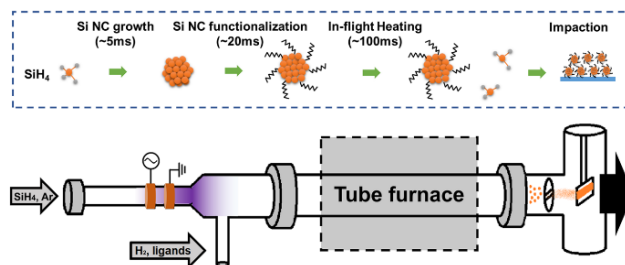


Fig. 1. Schematic of the experimental setup for this study.

The synthesis and functionalization setup is based on the design by Anthony *et al.* that is described in ref. [14]. A schematic of the experimental setup for this study is shown

in Fig. 1. Argon and silane (5% in helium) enter through a borosilicate glass tube reactor with ligands introduced into the plasma afterglow by flowing hydrogen through a bubbler to carry the ligands. Radiofrequency power at 13.56 MHz and a nominal value of 60 W was applied to a pair of copper ring electrodes placed 2 cm before the afterglow region. The argon flow rate varies between 30 and 100 sccm, and silane (5% in helium) and hydrogen flow rate were fixed at 14 sccm and 100 sccm, respectively. The gas pressure in the plasma region was 2.2–2.4 Torr. After the plasma region, the gas stream was sent through a 12-inch-long tube furnace with a parabolic temperature profile. Si NCs were collected onto glass substrates by inertial impaction using a setup similar to that used in ref. [9].

Si NCs were characterized using X-ray diffraction (XRD), dynamic light scattering (DLS), Fourier-transform infrared spectroscopy (FTIR). PLQY measurements were performed with an integrating sphere setup which is described in [9].

3. Results and Discussion

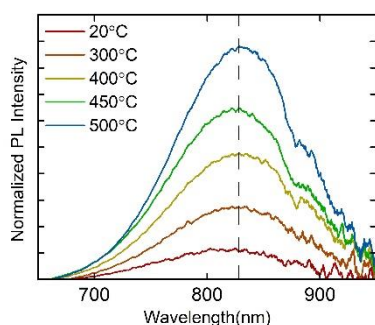


Fig. 2. Photoluminescence spectra (excitation $\lambda = 395$ nm) of 3.2 nm, 1-octene functionalized Si NC processed at different furnace temperatures. PL intensities are normalized with respect to integrated absorption, so the intensity shown is proportional to PLQY.

We observe a significant enhancement in PLQY when in-flight heating is applied. For PLQY studies, we synthesize Si NCs at 30 sccm of Ar flow rate, and the nanocrystal size estimated from XRD is 3.2 nm. For furnace temperatures from 20°C to 500°C (Fig. 2), the emission peaks are located at around 828 nm, with some minor sample-to-sample variances. The fact that the PL peak wavelengths remain constant implies that there is no shrinking of the Si NC core size associated with heating, as the photoluminescence of Si NCs originates from the nanocrystal core and is subject to quantum confinement effects. This indicates that the main role of heat treatment should be associated with modification of nanocrystal surfaces. In this temperature range, samples synthesized with increasing temperature exhibit increasing PLQY, reaching a maximum of 20% at 500°C. At 550°C, Si NCs no longer form a clear, stable solution in toluene, and PLQY also drops to ~15%. Both of these are likely the result of ligand dissociation at higher temperature.

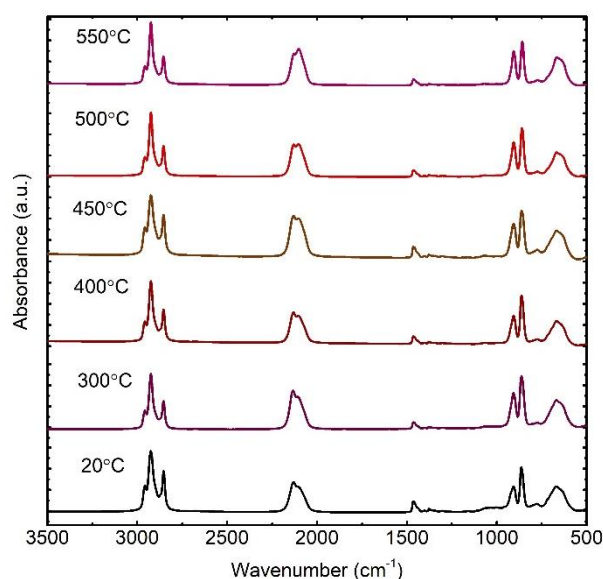


Fig. 3. FTIR spectra of Si NCs processed at various furnace temperatures.

Fig. 3 shows the Fourier-transform infrared spectroscopy (FTIR) spectra of 1-octene functionalized Si NCs with various furnace processing temperatures. FTIR measurements provide valuable information about surface group composition. The peaks between 2800–3000 cm^{-1} are assigned to CH_x ($x = 1-3$) stretching modes, and the feature between 2000–2200 cm^{-1} ($x = 1-3$) corresponds to SiH_x stretching modes of Si surface atoms that are not functionalized with a ligand. Therefore, the relative area ratio of the CH_x stretching region to the SiH_x stretching region (2000–2200 cm^{-1}) can qualitatively describe the surface ligand coverage. For a set of different furnace temperatures, including room temperature, the CH_x/SiH_x area ratios remain relatively constant, which indicates little differences in surface ligand coverage. This result indicates that although unreacted ligands can enter the furnace along with Si NCs, further ligand functionalization does not occur in the furnace. Ligand functionalization is essentially completed once the Si NCs leave the afterglow-plasma functionalization zone.

Previous studies suggested that thermal desorption of hydrogen [15,16] and changes of SiH_x species composition [17-19] can occur at the temperatures used here for in-flight heating of the SiNCs. Most relevant for this study, Shu *et al.* proposed that the desorption of hypervalent bonded SiH_3 is associated with an improvement in PLQY of plasma produced Si NCs [20]. Using first-principle calculations, the authors predicted fast non-radiative recombination that will lead to degraded PL in Si NCs which contain SiH_3 defects. A reduction of SiH_3 feature intensity at ~ 2141 cm^{-1} is observed as temperature increases, likely contributing to improved PLQY. We show that SiH_x species can significantly affect NC properties even in ligand-functionalized samples, as ligands only

partially cover the silicon surface due to steric hinderance and a significant amount of surface silicon atoms remain hydrogen terminated.

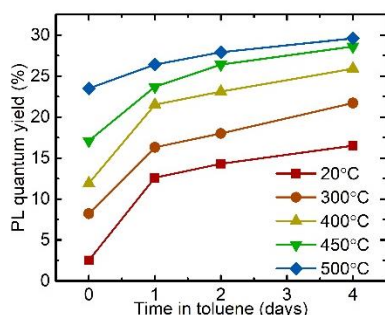


Fig. 4. The effect of aging on PLQY of 3.2 nm, 1-octene functionalized Si NCs processed at a series of furnace temperatures.

Potentially, PLQY of these gas-phase synthesized Si NCs can be even further improved, if we let the Si NCs age in an inert environment after synthesis. Fig. 4 shows the effect of aging on PLQY of samples processed at various furnace temperatures. As shown in Fig. 4, PLQYs slowly increase over time for all samples studied here. For the sample with 500°C furnace temperature, PLQY increases to 30% over 4 days. FTIR measurements show that this slowly increasing PLQY is concurrent with a further reduction in SiH₃ species. This result indicates that even in 500°C in-flight heated samples, a number of SiH₃ defect-containing particles due to nonadequate heating might still exist. Although the thermal equilibrium time of a single NC is very small, NCs will likely agglomerate as they enter the furnace after the plasma region and particles within an agglomerate might not be heated thoroughly. After synthesis, PLQY of these particles slowly increases due to silyl effusion, leading to an increase in overall sample PLQY.

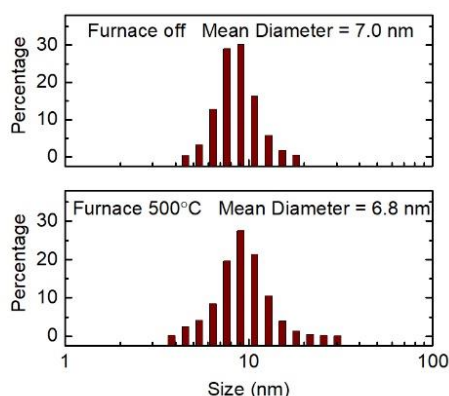


Fig. 5. Volume-weighted size distribution from DLS for samples produced without furnace heating and at 500°C furnace temperature.

While the all-gas-phase functionalization approach can be conveniently incorporated with gas-phase fabrication methods, we show that these Si NCs are also compatible with solution-based fabrication techniques as they are readily dispersible in common solvents. Dynamic light scattering (DLS) is performed to determine solubility of 1-dodecene functionalized Si NCs in toluene. Average hydrodynamic size of 500°C in-flight Si NCs is ~6.8 nm with a relatively narrow size distribution (Fig. 5). The result shows that the in-flight heating greatly enhances PLQY without compromising sample solubility.

4. Conclusions

Silicon nanocrystals with photoluminescence quantum yield above 20% and very good solubility in non-polar solvents have been synthesized via a one-step, all-gas-phase approach. The nanoparticles are synthesized in a nonthermal plasma and then functionalized in the plasma afterglow, followed by an in-flight heat treatment in a furnace. The plasma functionalization process produces a ligand-functionalized surface, which grants the Si NCs solubility in common nonpolar solvents. The in-flight heat treatment has a strong influence on the silicon-hydride groups at the Si NC surface and a close correlation between SiH_x group composition and sample PLQY is observed. The fact that Si NCs with respectable PLQY can be synthesized, functionalized, and heat treated entirely in the gas phase on time scales of ~100 ms represents an advance that may enable the practical application of Si NCs for many luminescent applications.

Acknowledgement

This work was supported in part by the National Institute of Health under award R01DA045549. Partial support is also acknowledged from DOE under the Energy Frontier Research Center for Advanced Solar Photophysics.

5. References

- [1] M. Francesco, S. Ehrenberg, L. Dharmo, F. Carulli, M. Mauri, F. Bruni, R. Simonutti, U. Kortshagen, S. Brovelli, *Nature Photonics*, **11**, 3 (2017).
- [2] K.Y. Cheng, R. Anthony, U.R. Kortshagen, R.J. Holmes, *Nano Letters*, **11**, 5 (2011).
- [3] P.D. Puzzo, E.J. Henderson, M.G. Helander, Z. Wang, G.A. Ozin, Z. Lu, *Nano Letters*, **11**, 4 (2011).
- [4] W.W. Yu, E. Chang, R. Drezek, and V.L. Colvin, *Biochemical and Biophysical Research Communications*, **348**, 3 (2006).
- [5] E.J. Henderson, A.J. Shuhendler, P. Prasad, V. Baumann, F. Maier-Flaig, D.O. Faulkner, U. Lemmer, X.Y. Wu, G.A. Ozin, *Small*, **7**, 17 (2011).
- [6] F. Erogbogbo, K. T. Yong, I. Roy, R. Hu, W. C. Law, W. Zhao, H. Ding, F. Wu, R. Kumar, M. T. Swihart, P. N. Prasad, *ACS Nano*, **5**, 1 (2010).
- [7] S. Pramanik, S. K. Hill, B. Zhi, N. V. Hudson-Smith, J. J. Wu, J. N. White, E. A. McIntire, V.S.K. Kondeti,

- A.L. Lee, P.J. Bruggeman, U.R. Kortshagen, *Environmental Science: Nano*, **5**, 8 (2018).
- [8] L. Mangolini, E. Thimsen, and U. Kortshagen, *Nano Letters*, **5**, 4 (2005).
- [9] D. Jurbergs, U. Kortshagen, *Applied Physics Letters*, **88**, 23 (2006).
- [10] M. P. Stewart, J. M. Buriak, *Journal of the American Chemical Society*, **123**, 32 (2001).
- [11] P.K. Tapas, M. Iqbal, M.H. Wahl, K. Gottschling, C.M. Gonzalez, M.A. Islam, J.G.C. Veinot, *Journal of the American Chemical Society*, **136**, 52 (2014).
- [12] Y. Yu, C.M. Hessel, T.D. Bogart, M.G. Panthani, M.R. Rasch, and B.A. Korgel, *Langmuir*, **29**, 5 (2013).
- [13] L. Mangolini, U. Kortshagen, *Advanced Materials*, **19**, 18 (2007).
- [14] R.J. Anthony, K.Y. Cheng, Z.C. Holman, R. J. Holmes, U.R. Kortshagen, *Nano Letters*, **12**, 6 (2012).
- [15] J. Holm, J.T. Roberts, *Journal of the American Chemical Society*, **129**, 9 (2007).
- [16] J. Holm, J.T. Roberts, *Journal of Vacuum Science & Technology A: Vacuum, Surfaces, and Films*, **28**, 2 (2010).
- [17] N. Salivati, J.G. Ekerdt, *Surface Science*, **603**, 8 (2009).
- [18] B.N. Jariwala, N. Bhavin, N.J. Kramer, M.C. Petcu, D.C. Bobela, MCM van de Sanden, P. Stradins, C.V. Ciobanu, and S. Agarwal, *The Journal of Physical Chemistry C*, **115**, 42 (2011).
- [19] L.M. Wheeler, N.C. Anderson, P.K.B. Palomaki, J.L. Blackburn, J.C. Johnson, N.R. Neale, *Chemistry of Materials*, **27**, 19 (2015).
- [20] Y. Shu, U.R. Kortshagen, B.G. Levine, R.J. Anthony, *The Journal of Physical Chemistry C*, **119**, 47 (2015).